Development 133, 21-32 doi:10.1242/dev.02160

p38 MAPK is essential for secondary axis specification and patterning in sea urchin embryos

Cynthia A. Bradham and David R. McClay*

Most eggs in the animal kingdom establish a primary, animal-vegetal axis maternally, and specify the remaining two axes during development. In sea urchin embryos, the expression of Nodal on the oral (ventral) side of the embryo is the first known molecular determinant of the oral-aboral axis (the embryonic dorsoventral axis), and is crucial for specification of the oral territory. We show that p38 MAPK acts upstream of Nodal and is required for Nodal expression in the oral territory. p38 is uniformly activated early in development, but, for a short interval at late blastula stage, is asymmetrically inactivated in future aboral nuclei. Experiments show that this transient asymmetry of p38 activation corresponds temporally to both oral specification and the onset of oral Nodal expression. Uniform inhibition of p38 prevents Nodal expression and axis specification, resulting in aboralized embryos. Nodal and its target Gsc each rescue oral-aboral specification and patterning when expressed asymmetrically in p38-inhibited embryos. Thus, our results indicate that p38 is required for oral specification through its promotion of Nodal expression in the oral territory.

KEY WORDS: p38, Embryonic axis, Nodal, Gsc

INTRODUCTION

Axis specification and patterning is a foundational developmental process, during which the hierarchical specification of increasingly smaller and more specialized territories ultimately produces the three-dimensional animal. The primary embryonic axis, the anteroposterior or animal-vegetal axis, is usually specified by maternal mechanisms, while asymmetries that arise after fertilization establish the dorsoventral (DV) and left-right (LR) axes. One of the signals frequently employed during axis specification is Nodal (Schier and Shen, 2000), which is often involved in the patterning of multiple axes. In the sea urchin embryo, Nodal first specifies the oral (ventral) territory along the oral/aboral (embryonic DV) axis (Duboc et al., 2004; Flowers et al., 2004), and then is later employed during LR axis specification (Duboc et al., 2005).

The sea urchin embryo develops into a bilaterally symmetric pluteus larva with a three-part gut and a skeleton. The animal-vegetal axis is maternally established, and consequent post-fertilization events lead to asymmetrical β-catenin nuclearization in the vegetal territory. β-catenin in turn initiates an endomesodermal gene regulatory network (GRN) that establishes the vegetal embryonic territories (Logan et al., 1999; Davidson et al., 2002). By contrast, the oral/aboral (OA) axis is not maternally determined, as isolated blastomeres from 2- or 4-cell embryos develop into small but otherwise normal larvae (Driesch, 1892; Cameron et al., 1996). Specification of the OA axis also depends on β-catenin nuclearization (Wikramanayake et al., 1998; Logan et al., 1999), although this is might be an indirect requirement, reflecting a need for prior induction of the endomesodermal GRN to initiate OA specification.

Nodal is the earliest known protein capable of inducing oral specification. Nodal is upstream from the transcriptional repressor Gsc, which is functionally implicated as regulator of oral specification (Angerer et al., 2001). Gsc is upstream from the oral transcriptional activator Deadringer (Dri), and represses the aboral transcription factor Tbx2/3 (Amore et al., 2003; Croce et al., 2003; Duboc et al., 2004). The initial asymmetry that eventually induces Nodal expression in the oral territory is unknown, although the asymmetrical distribution of mitochondria along the OA axis is a strong candidate (Coffman et al., 2004). Nodal is expressed on the oral side of the embryo, which is enriched in mitochondria; furthermore, embryos cultured under hypoxic conditions fail to express Nodal (Coffman et al., 2004), suggesting a causal role for redox potential. Mitochondrial-derived reactive oxygen intermediates have been previously shown to activate p38 MAPK (Ushio-Fukai et al., 1998; Kulisz et al., 2002; Lee et al., 2002), a protein kinase known to participate in axis specification or tissue polarization in various organisms (Suzanne et al., 1999; Fujii et al., 2000; Goswami et al., 2001).

MAPKs are divided into two families: growth factor-activated (ERK) and stress-activated kinases (JNK and p38). Although identified as a stress responder, p38 conveys a variety of signals, including conventional growth, migratory and death signals, as well as responding to environmental and mechanical stimuli, such as UV light, hyperosmolarity and redox changes (Shi and Gaestel, 2002). These signals induce phosphorylation of p38, which triggers both its translocation to the nucleus and the activation of its catalytic function. This transduction mechanism is distinct from that of other signaling pathways, in which transcription factors rather than kinases relocate from the cytoplasm to the nucleus, for example β-catenin, SMADs, and NFκB. This is clearly an ancient and important means of signaling, as MAPKs are well conserved from yeast to mammals. The purpose of this study was to determine the role of p38 MAPK in sea urchin development. The results show that p38 is required for both OA specification and Nodal expression.

MATERIALS AND METHODS

Lvp38 cloning and mutagenesis

A fragment of Lvp38 obtained by degenerate PCR was used to probe an Lv phage library, which produced a partial p38 cDNA. A full-length clone (GenBank Accession Number AY445029) was obtained using 3′ RACE (Clontech). Kinase-inactive p38 (T183A, Y185F) was generated using the QuikChange Mutagenesis Kit (Stratagene). A C-terminal EGFP fusion was produced by eliminating the stop codon in Lvp38 and adding the coding sequence of EGFP (Clontech) in frame.

DCBM Group, Biology Department, Duke University, Durham, NC 27708, USA

*Author for correspondence (e-mail: dmcclay@duke.edu)

Accepted 12 October 2005

Macroarray, subtractive hybridization and LvGsc cloning

A *Lytechinus variegatus* midgastrula cDNA phage library was excised in bulk to provide bacterial colonies for the macroarray, which was produced using the QBOT robot at the Beckman Institute (Caltech, Pasadena, CA), as described previously (Rast et al., 2000). PolyA-selected RNA from mesenchyme blastula-stage control and SB-treated embryos was used for the subtractive hybridization, which was performed as described previously (Rast et al., 2000). Macroarray filters were probed before and after subtraction. Clones enriched after subtraction were sequenced and subjected to BLAST searching for identification. A full-length clone of LvGsc was identified (Accession Number AY445030), and the ORF was subcloned for mRNA synthesis.

LvNodal cloning

Low degeneracy primers obtained by comparison of the ORFs for *Paracentrotus lividus* Nodal (PlNodal) (Duboc et al., 2004) and *Strongylocentrotus purpuratus* Nodal (SpNodal) (provided by T. Lepage) were used to amplify a 1 kb fragment of *L. variegatus* Nodal (LvNodal). The full-length LvNodal (Accession Number DQ017963) was obtained by 5′ and 3′ RACE (Ambion).

Other constructs

A partial clone of LvDri was identified in the subtraction screen. A plasmid encoding human MKK6E was provided by Dr P. Scherer, and the insert was subcloned into pCS2 for mRNA synthesis.

Animals, injections and drug treatments

L. variegatus adults were obtained from Susan Decker (Hollywood, FL), Sea Life (Tavernier, FL), or from the Duke University Marine Laboratory at Beaufort, NC. Gametes were harvested, cultured and injected by standard methods. For 2-cell stage injections, rhodamine-conjugated dextran was co-injected to label the injected cell. mRNA was transcribed in vitro using the mMessage mMachine Kit (Ambion). LvNodal-specific MASO (sequence TGCATGGTTAAAAGTCCTTAGAGAT) was obtained from Gene Tools. SB203580 (SB) was obtained from Calbiochem. SB (20 μM) was added to cultures during early cleavage stages, unless otherwise noted. Treatment with DMSO vehicle had no effect (not shown). Doses for these reagents were determined by dose-response experiments.

In situ hybridization

In situ hybridization was performed using standard methods, with DIG-labeled full-length RNA probes and NBT/BCIP or BM purple colorization (Roche). Hybridizations and washes were carried out at 65°C.

Immunostaining

Embryos were fixed, stained and imaged as described (Gross et al., 2003), using CY3-labeled secondary antibodies (Jackson Laboratories) and PBS+0.1% Tween 20 throughout.

Western blotting

Total cell lysate (100 μg) was separated by electrophoresis on 10% SDS-PAGE gels, then transferred to nitrocellulose membranes and probed, as described previously (Bradham et al., 1998).

P-p38 staining

Embryos were fixed in 2% paraformaldehyde, 25 mg/ml sodium periodate, 135 mg/ml lysine, 18 mM Na_2HPO_4, 20 μM β-glycerophosphate, 10 μM 2-nitrophenylphosphate and 50 μM sodium orthovanadate in sea water, then permeablized in PBS+0.1% Triton X-100. Staining was performed as described (Gross et al., 2003). Embryos were incubated in primary antibody at a dilution of 1:10 (P-p38, Cell Signaling Technology), and PBS+0.1% Triton X-100 was used throughout. Hoechst's dye (Molecular Probes) was included in the final wash at 10 μg/ml.

DiI labeling and live confocal microscopy

DiI (C18, Molecular Probes) was transferred to blastomeres at the 4-cell stage by iontophoresis, as described previously (Logan and McClay, 1997). For live imaging, embryos were sealed between protamine sulfate-coated glass slides and coverslips filled with sea water, then imaged using confocal microscopy with *z*-series images collected at 10-minute intervals.

QPCR analysis

Total RNA was prepared from 10 embryos using Trizol (Invitrogen) and glycogen carrier (Ambion). The sample was used for reverse transcriptase (RT) reactions with Taqman RT-PCR kits (Applied Biosystems) after pretreatment with DNase I (DNA-*free*, Ambion). QPCRs were performed using a LightCycler Instrument and a Fast Start SYBR Green PCR Kit (Roche). Results were calculated by subtracting the sample C_T (crossing point threshold) from the control C_T to determine ΔC_T, then normalizing to ubiquitin.

RESULTS

Lvp38 MAPK is highly conserved and continuously expressed during sea urchin development

To investigate the role of p38 in sea urchin development, Lvp38 MAPK was cloned from an *Lytechinus variegatus* midgastrula cDNA library. The Lvp38 protein is 66% identical and 73% similar to human p38 (Fig. 1A), and 41% identical to yeast HOG1 (not shown). In particular, the phosphorylation motif TGY (residues 183-185, Fig. 1A, blue box) is identical, and the surrounding amino acids are well conserved. Phylogenetic analysis indicated that Lvp38 clusters with the vertebrate p38 α and β subtypes, rather than the γ and δ subtypes (not shown).

MAPKs are typically regulated not by transcriptional control, but rather by phosphorylation. Not surprisingly, QPCR analysis of Lvp38 indicated that relative p38 mRNA levels vary by less than twofold from the egg to the hatched blastula stage, with moderately higher levels expressed at later stages (data not shown). Overexpression of wild-type p38 had no effect on development (not shown), as expected for a protein regulated by post-translational mechanisms.

Inhibition of p38 activity blocks oral-aboral but not endomesodermal specification

Like all MAPKs, p38 is activated by phosphorylation on conserved T and Y residues. Dominant-negative Lvp38 was generated by mutating the phosphoacceptor motif TGY to AGF to produce kinase-inactive (KI) p38. These mutations effectively block mammalian p38 activation (Raingeaud et al., 1995). In parallel, the well-established, highly specific p38 inhibitor SB203580 (SB) (Tong et al., 1997; Davies et al., 2000) was used to inhibit p38 activity. Extensive characterization has shown that SB is among the most specific of the kinase inhibitors currently available (Davies et al., 2000); this specificity is illustrated by the fact that mammalian p38 was independently identified on the basis of binding to SB (Lee et al., 1994).

SB binds to the ATP-binding pocket of human p38 (Young et al., 1997). The crystal structure of human p38 complexed with SB shows that nine residues specifically interact with SB (Wang et al., 1998). Of those nine residues, seven are identical in Lvp38, while an additional residue is similar (Fig. 1A, green boxes). The dissimilar residue (His 107) forms only secondary contacts with SB (Wang et al., 1998). SB also makes non-specific contacts (i.e. hydrophobic and van der Waal's contacts) with five β-sheets and one α-helix in human p38 (Wang et al., 1998). The alignment shows that these elements are 80% identical and 83% similar in Lvp38 (Fig. 1A, gray boxes), suggesting that SB is likely to interact similarly with Lvp38 and human p38.

Activating mutants of p38 have not been described; in tissue culture systems, constitutive activation of the p38 pathway is often accomplished by the expression of activated MKK6, a kinase immediately upstream from p38 (Raingeaud et al., 1996). Unfortunately, attempts to inject mRNA encoding activated MKK6

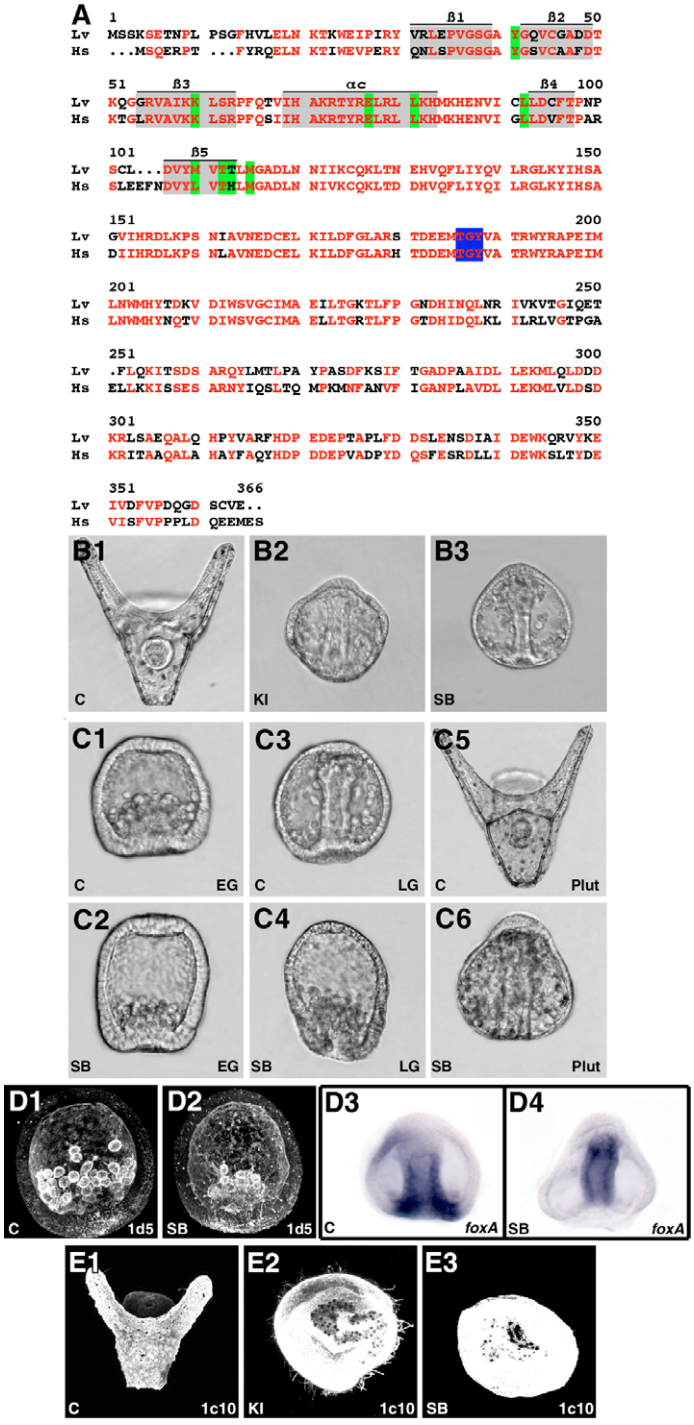

Fig. 1. Lvp38 inhibition specifically blocks oral specification. (**A**) Alignment of Lvp38 (Lv) and human p38 (Hs). Residues that are identical or 90% similar (Corpet, 1988) are indicated in red. The phosphorylation motif TGY is labeled blue. Specific SB-interacting residues are labeled green, and non-specific SB-interacting structural elements are labeled gray. (**B**) Brightfield images are shown of control (B1), KI p38-expressing (1.4 pg/pl, B2) and SB-treated (20 μM, B3) embryos. (**C**) Control (top) and SB-treated (bottom) embryos shown at early gastrula (C1,C2), late gastrula (C3,C4) and pluteus stages (C5,C6). (**D**) D1 and D2 show immunostaining of PMCs with 1d5 at the mesenchyme blastula stage in control (D1) and SB-treated (D2) embryos. Images are full projections of confocal *z*-series. (D3,D4) Whole-mount in situ analysis of FoxA in control (D3, late gastrula) and SB-treated (D4, pluteus stage) embryos, shown in lateral views. (**E**) Control (E1), KI p38-expressing (E2) and SB-treated (E3) embryos were immunolabeled with the aboral marker 1c10 at pluteus stage. Full projections are shown.

resulted in the rapid death of embryos across a wide range of mRNA doses (ranging to 0.001 pg/pl, not shown). This suggests that precocious activation of p38 is not compatible with survival.

Inhibition of p38 resulted in embryos that lacked skeletons (Fig. 1B). This effect was observed in both KI-injected embryos (Fig. 1B2) and SB-treated embryos (Fig. 1B3). The skeleton is secreted by the primary mesenchyme cells (PMCs), which ingress from the vegetal plate at mesenchyme blastula stage. In SB-treated embryos, the ingression of PMCs occurred with normal timing based on morphology (Fig. 1C1,C2); immunostaining with the PMC marker 1d5 confirmed that PMCs differentiated normally in the absence of p38 activity (Fig. 1D1,D2). Thus, p38 is not required for the ingression or differentiation of PMCs.

PMC ingression is followed by the invagination of the archenteron. Morphological assessment shows that invagination was delayed in SB-treated embryos (Fig. 1C3,C4), but was completed at the pluteus stage (Fig. 1C5,C6), at which point the SB-treated embryos resembled normal late-gastrula stage embryos (Fig. 1C3). Both control and SB-treated embryos expressed FoxA in the endodermal compartment (Fig. 1D3,D4), indicating that p38 is not required for endoderm specification or invagination movements. Secondary mesenchyme cells (SMCs) are localized at the invaginating tip of the archenteron and delaminate from the archenteron during gastrulation, giving rise to various cell types including pigment cells. KI-injected (not shown) and SB-treated embryos were pigmented (see Fig. 2A2), indicating that p38 is not required for SMC specification and differentiation. Together, these results indicate the p38 does not play a role in endomesoderm specification or differentiation.

To assess the ectoderm, embryos were labeled with the aboral marker 1c10 (Fig. 1E). Both KI-overexpressing (Fig. 1E2) and SB-treated embryos (Fig. 1E3) expressed the 1c10 antigen uniformly and robustly, suggesting that such embryos are aboralized. This contention is strengthened by the observation that the oral stomadeal component of FoxA expression is absent in SB-treated embryos (Fig. 1D3,D4). Together, these data suggest that p38 activity is specifically required for skeletogenesis and for the establishment of the oral territory.

p38 activity is required for expression of oral-specific genes

Because p38 inhibition resulted in aboralization, the relationship between p38 and known oral-specific genes was assessed (Fig. 2). *L. variegatus* clones of Nodal (LvNod) and Goosecoid (LvGsc) were obtained. The Tgfβ family member LvNod encoded a protein 71.6% and 74.6% identical to PlNod and SpNod proteins, respectively, whereas the mature cleaved form is 86.9% and 82.5% identical, respectively, to PlNod and SpNod. LvGsc was independently identified in a subtraction screen as a p38 target gene. LvGsc protein is 83% identical to SpGsc.

Overexpression of LvNod (Fig. 2A3) and LvGsc (Fig. 2A4) produced phenotypes consistent with those previously published in other sea urchin species (Angerer et al., 2001; Duboc et al., 2004;

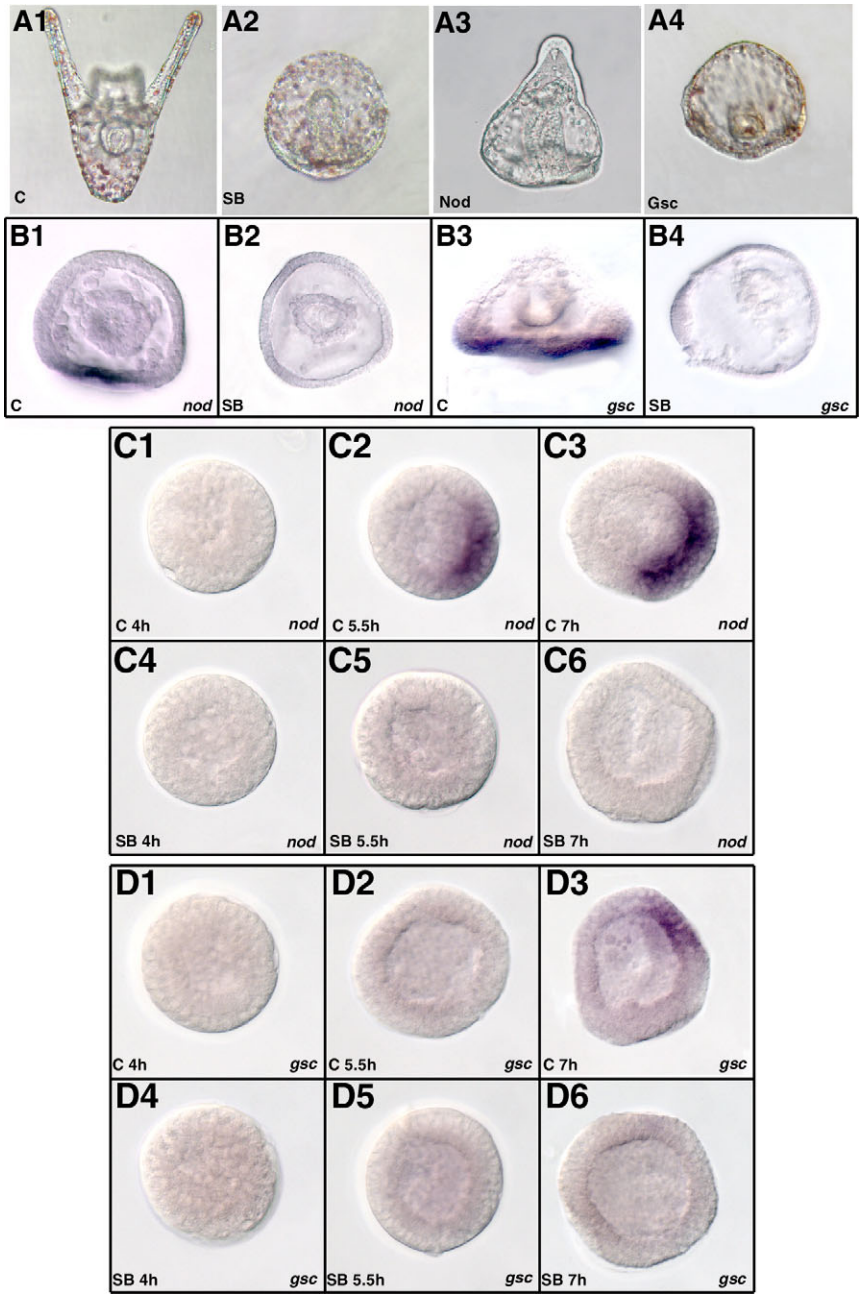

Fig. 2. p38 is required for the expression of Nodal (Nod) and Goosecoid (Gsc). (**A**) Brightfield or DIC images of control (A1), SB-treated (A2), LvNod-overexpressing (A3) and LvGsc-overexpressing (A4) embryos. Doses were 0.2 pg/pl for LvNod and 0.05 pg/pl for LvGsc mRNA. (**B**) Whole-mount in situ analysis in control (B1,B3) and SB-treated (B2,B4) embryos for LvNod (B1,B2, late gastrula) and LvGsc (B3,B4, prism), shown in vegetal views. (**C**,**D**) Whole-mount in situ analysis for Nodal (C) and Gsc (D) in control (top) and SB-treated (bottom) embryos at early blastula (4h, left), late blastula (5.5h, middle) and hatched blastula (7h, right).

Flowers et al., 2004). Whole-mount in situ analysis showed no expression of LvNod or LvGsc in SB-treated embryos (Fig. 2B). KI-p38 expression also significantly inhibited both Nodal and Gsc expression, as assessed by QPCR analysis (not shown). Thus, p38 activity is required for the expression of both Nodal and Gsc at late embryonic stages.

To test whether p38 activity is required for the transcriptional initiation of these genes, whole-mount in situ analysis for LvNod (Fig. 2C) and LvGsc (Fig. 2D) was performed at earlier timepoints. The results show that, in *L. variegatus* embryos, Nodal expression begins at 5.5 hours post-fertilization (hpf), at late blastula stage (Fig. 2C1-C3), whereas Gsc expression begins at 7 hpf, at hatched blastula stage (Fig. 2D1-D3), consistent with Nodal acting upstream of Gsc. SB treatment abrogated the expression of both genes (Fig. 2C4-C6,D4-D6). Thus, p38 activity is required for the initiation of both Nodal and Gsc transcription.

Late blastula stage is the end point of the p38 requirement for oral specification

To evaluate the timing of p38 activation, embryos were treated with SB at different stages, then cultured to the pluteus larva stage and assessed (Fig. 3A). These experiments are based on the logic that once p38 has activated its targets, addition of the inhibitor will have no further effect. Addition of SB up to hatched blastula stage (7 hpf) blocked skeletogenesis (Fig. 3B1,B2), whereas later addition of SB had no effect (Fig. 3B3,B4). These results indicate that the requirement for p38 activity extends to the hatched blastula stage with respect to skeletogenesis.

Comparison of embryos inhibited at early blastula and hatched blastula shows a subtle difference in morphology, as embryos treated at early blastula display a completely radialized phenotype (Fig. 3B1), whereas embryos treated at hatched blastula (Fig. 3B2) show some OA character, as indicated by the asymmetrical

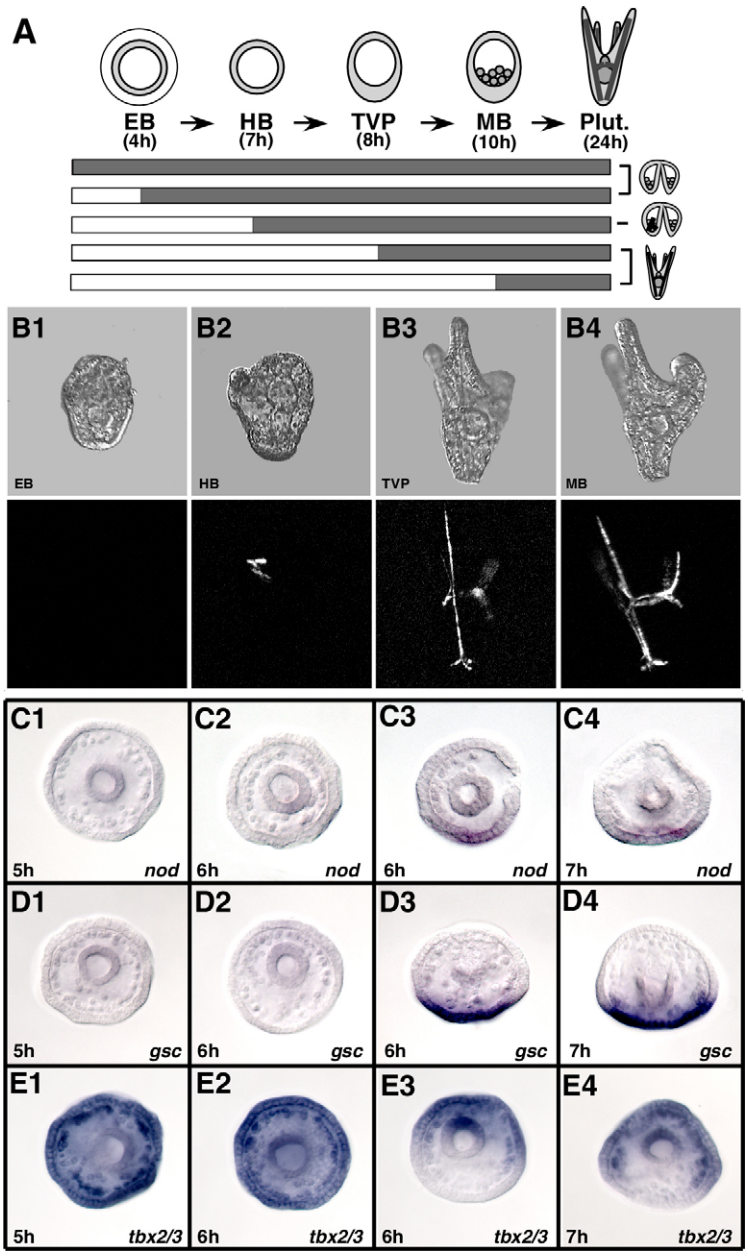

Fig. 3. p38 is required for oral specification at late blastula stage. (**A**) Schematic depicting the experiment in B. Corresponding hours post-fertilization (h) are indicated. (**B**) Embryos were treated with SB at the indicated stages (B1-B4), and then cultured to the pluteus stage. Morphological (top) and skeletal (bottom, illuminated with plane-polarized light) images are shown. (**C**-**E**) Whole-mount in situ analysis for Nodal (C), Gsc (D) and Tbx2/3 (E) in embryos treated with SB at 5 (1), 6 (2,3) and 7 (4) hpf. Vegetal views at late gastrula stage are shown. EB, early blastula; HB, hatched blastula; TVP, thickened vegetal plate; MB, mesenchyme blastula; Plut, pluteus larvae.

appearance of both skeletal initiations and arm buds. This suggested that p38 inhibition at early blastula blocked OA axis specification, whereas inhibition at hatched blastula did not.

This proposition was tested using whole-mount in situ analysis. Embryos were treated with SB at hourly intervals to the thickened vegetal plate stage, then cultured to late gastrula stage when they were fixed and evaluated. SB addition at 5 hpf (early blastula stage) blocked the expression of Nodal and Gsc (Fig. 3C1,D1), and resulted in the uniform expression of the aboral transcription factor Tbx2/3 (Fig. 3E1). By contrast, addition of SB at 7 hpf (hatched blastula stage) had no impact on the normal expression patterns for either of the oral genes Nodal and Gsc (Fig. 3C4,D4), or aboral Tbx2/3 (Fig. 3E4). SB treatment at 6 hpf (late blastula stage) resulted in a mixture of both phenotypes, indicating that 6 hpf is the endpoint for p38 function with respect to oral specification. The mixture of phenotypes probably reflects the normal asynchrony of the culture. The 6 hpf timepoint corresponds reasonably well with the onset of Nodal expression at 5.5 hpf (Fig. 2C2). These results show that the effects of p38 on oral specification and skeletogenesis are separable temporally, as oral specification occurs at 6 hpf, whereas the skeletogenic requirement for p38 activity extends to at least 7 hpf. For this study, the focus remained on the earlier event, oral specification.

SB removal reveals a patterning defect

To test the reversibility of p38 inhibition, SB-treated embryos were washed from the inhibitor at different timepoints and the embryos were cultured to the pluteus stage (Fig. 4A). When SB was removed prior to the mesenchyme blastula stage, normal pluteus larvae were produced, demonstrating that SB treatment is reversible. However, washouts at or after the mesenchyme blastula stage (‘SB-wash’) resulted in embryos with abnormal skeletal patterning (Fig. 4B). The patterning defects were dramatic, with each embryo showing a unique pattern (Fig. 4B2,B3, compare with

Fig. 1A1). Such skeletal patterning defects are characteristic of OA axial defects (Hardin et al., 1992; Croce et al., 2003; Gross et al., 2003), because, although the skeleton is secreted by the PMCs, the skeletal pattern arises in response to spatial cues within the ectoderm (Armstrong et al., 1993; Malinda and Ettensohn, 1994). Thus, the patterning defects are again consistent with p38 functioning in OA axis specification. Quantitation of the washout experiments demonstrates that the change from normal to abnormal recovery occurred abruptly at the mesenchyme blastula stage (Fig. 4B1). At first glance, these results might suggest that p38 activity is still important for OA specification at mesenchyme blastula stage; however, the timecourse data in Fig. 3 show that addition of SB at mesenchyme blastula has no effect, indicating that p38 activity is unnecessary at this stage (Fig. 3B4). Thus, although the consequences of p38 inhibition become irreversible at mesenchyme blastula, p38 activity itself is no longer required at this stage.

One explanation for these observations is that Nodal and Gsc expression recover once SB is removed, but with removal at and after mesenchyme blastula, the recovery is too slow to restore normal axial patterning. Accordingly, the recovery of Nodal and Gsc expression in SB-wash embryos was assessed by QPCR analysis (Fig. 4C). Nodal expression in controls is biphasic, with reduced levels at late gastrula stage, consistent with results in *P. lividus* embryos (Duboc et al., 2004) (Fig. 4C1). Gsc expression increases steadily from hatched blastula to pluteus stage in control embryos (Fig. 4C2). SB treatment significantly inhibited both Nodal and Gsc expression (Fig. 4C1,C2), consistent with the in situ results. Nodal recovered quickly to control levels in SB-wash embryos (Fig. 4C1), but Gsc recovered more slowly, and did not return to control levels until the pluteus stage (Fig. 4C2). This is consistent with the explanation that in SB-wash embryos, the recovery of Gsc expression is too late to restore normal OA specification and the consequent skeletal patterning.

p38 is active only on the oral side at late blastula

To measure the activation of p38, a phospho-specific antibody was employed. Phosphorylation of p38 triggers both activation of its kinase function and translocation of the protein to the nucleus (Raingeaud et al., 1995; Fujii et al., 2000; Shi and Gaestel, 2002). The antibody detects only the phosphorylated, and thus only the activated, form of the protein. Comparison of the primary sequence of human and *L. variegatus* p38 (Fig. 1A) shows that that the phosphorylation site and the surrounding residues are identical in the two species, indicating that the phospho-specific antibody is likely to cross-react with Lvp38. Indeed, western blot analysis indicated that anti-phospho-p38 (P-p38) antibody labeled a single band of the expected molecular weight (Fig. 5A). The results show that p38 becomes activated at the 60-cell stage, and remains active throughout development at low levels (Fig. 5A). Unfortunately, commercial antibodies recognizing total p38 protein did not cross-react with Lvp38 (not shown).

The phospho-specific antibody was next used to assess the spatial localization of activated p38 (Fig. 5B). Uniform nuclear P-p38 staining was observed as early as the 60-cell stage, consistent with the western blot data (not shown). Prior to 5.5 hpf (late blastula stage), P-p38 was present in all nuclei (Fig. 5B1). At 5.5 hpf, P-p38 was cleared from nuclei on one side of the embryo (Fig. 5B2). Forty-five minutes later, P-p38 had recovered its ubiquitous distribution (Fig. 5B3). Nuclear staining with Hoechst's dye (Fig. 5B4-B6) confirmed that the P-p38 nuclear clearance did not reflect a nuclear disruption or a visualization artifact. The cleared area arose at late blastula stage and persisted for less than one hour. Thus, p38 activity is spatially asymmetric for a brief interval corresponding to the late blastula stage.

To independently corroborate this observation, a Lvp38-EGFP fusion construct (p38-GFP) was employed to permit the live imaging of p38 activity in the embryo as a function of nuclear localization, as the activated kinase is nuclear, whereas the inactive kinase is

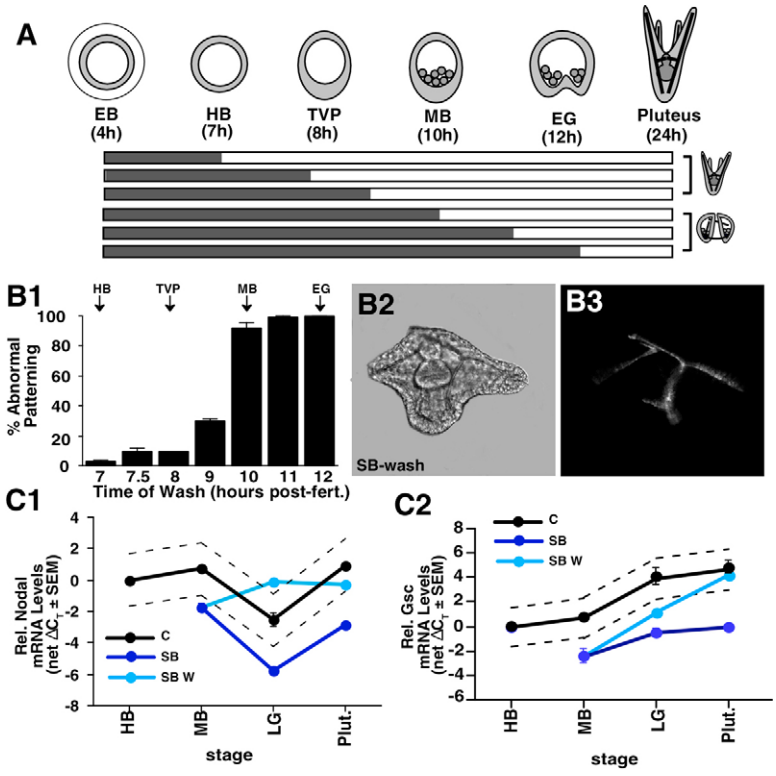

Fig. 4. SB removal reveals OA patterning defects. (**A**) Schematic depicting the experiment in B. (**B**) In B1, data are expressed as the percentage of embryos with abnormal patterning ±s.e.m. following SB-wash at various time points. Corresponding stages are indicated above the graph. (B2,B3) Phenotype of SB-wash embryos, illuminated with brightfield (B2) and plane-polarized light (B3). (**C**) QPCR analysis for Nodal (C1) and Gsc (C2) relative expression levels in control, SB-treated and SB-wash embryos. Data are expressed as net ΔC_T±s.e.m., with controls at hatched blastula (HB) arbitrarily set to zero. Dashed lines indicate the threshold for significance. EG, early gastrula; LG, late gastrula.

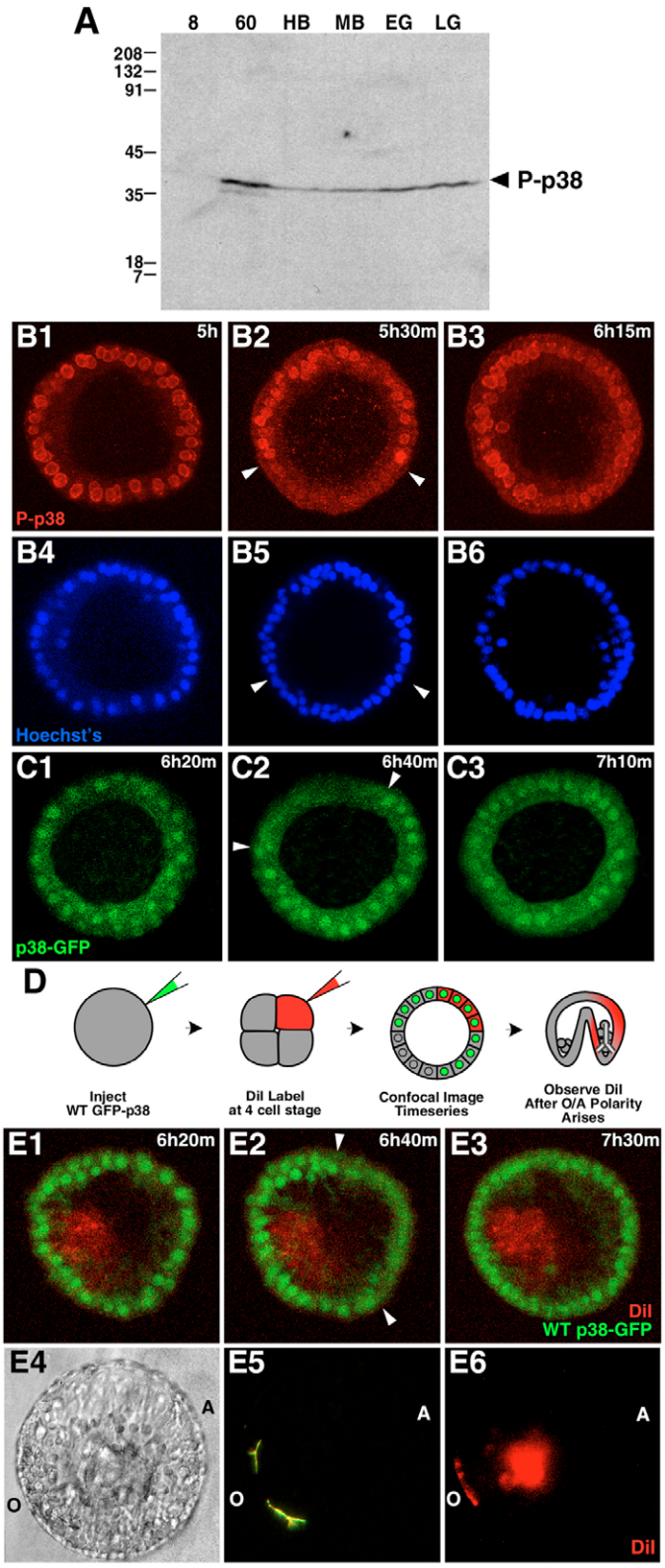

Fig. 5. p38 is transiently inactivated on the future aboral side of the embryo. (**A**) Western blot analysis for phospho-p38 at the indicated stages. P-p38 is indicated by an arrowhead. 8, 8 cell; 60, 60 cell. (**B**) Embryos stained with anti-P-p38 antibody (B1-B3) and Hoechst's dye (B4-B6) at the indicated timepoints post-fertilization. The cleared region is indicated by arrowheads. Images are internal projections of 10 sections from a confocal *z*-series. (**C**) A single embryo expressing Lvp38-GFP (0.015 pg/pl), imaged using a live confocal timecourse, is shown at the indicated timepoints post-fertilization (C1-C3). The cleared region is indicated by arrowheads. Images are internal projections of 20 sections. (**D**) Schematic depicting the experimental approach used in E. (**E**) A similar embryo to the one in C, but also labeled with DiI (red). (E1-E3) Internal projections of 25 sections at the indicated hpf. (E4-E6) The same embryo at late gastrula stage, with morphology (E4), skeleton (E5) and DiI labels shown (E6). The oral (O) and aboral (A) poles are indicated.

cytoplasmic. Embryos expressing p38-GFP developed normally (not shown). Live confocal timecourse experiments showed that p38-GFP was transiently cleared from nuclei on one side of the embryo, confirming the staining results above (n=8/10, Fig. 5C). In these experiments, the cleared area persisted for an interval ranging from 30 to 50 minutes. The difference in timing for the onset of clearance in panels B and C reflects the developmental delay caused by microinjection. In both cases, the cleared area arose at 90 minutes prior to hatching.

There are no landmarks at blastula stages to indicate the developmental fate of the cleared region. To address this question, p38-GFP was used in combination with a cell lineage tracer (Fig. 5D). To track the fate of the cleared region, eggs were first injected with p38-GFP mRNA, then, at the 4-cell stage, one blastomere was labeled with DiI by iontophoresis. In each experiment, a single embryo was serially imaged over a 3-hour period encompassing the late blastula stage to visualize the spatial relationship between the nuclear clearance of p38 and the DiI label. The embryo was then cultured until OA polarization was detectable, at which point the location of the DiI label permitted an assessment of the fate of the cleared region (Fig. 5D). An example is shown in Fig. 5E. In this embryo, p38-GFP was transiently cleared from nuclei on the side opposite to the DiI label (Fig. 5E2). After development to the gastrula stage, the DiI label was distributed to both the gut and the ectoderm, with the ectodermal component localized to the same side as the triradiate spicules (Fig. 5E5,E6), and thus to the oral region. Based on that landmark, the cleared region in Fig. 5E2 was the future aboral side of the embryo. The cleared region corresponded to the aboral ectoderm in three out of three cases in which the DiI label provided an unambiguous axis orientation. Together, these data show that p38 is transiently inactivated on the aboral side of the embryo at late blastula stage, and thus is active only on the future oral side during an interval that is coincident with both the onset of Nodal expression (Fig. 2C) and p38-dependent oral specification (Fig. 3C-E).

Nodal and Gsc oralize embryos downstream from p38

LvNod expression begins at late blastula stage, which is the same stage that the asymmetric p38 clearance was observed. Although the evidence suggested that p38 is upstream from Nodal, it was also possible that Nodal participates in regulating the clearance of p38 in a feedback loop. If true, oral Nodal would provide an inducing function to maintain oral p38 activation, and in the absence of Nodal, p38 would be expected to be cleared uniformly. To test this possibility, a morpholino-substituted antisense oligonucleotide (MASO) directed against LvNod (Nod MASO) was employed (Fig. 6A). Injection of Nod MASO induced morphological perturbations

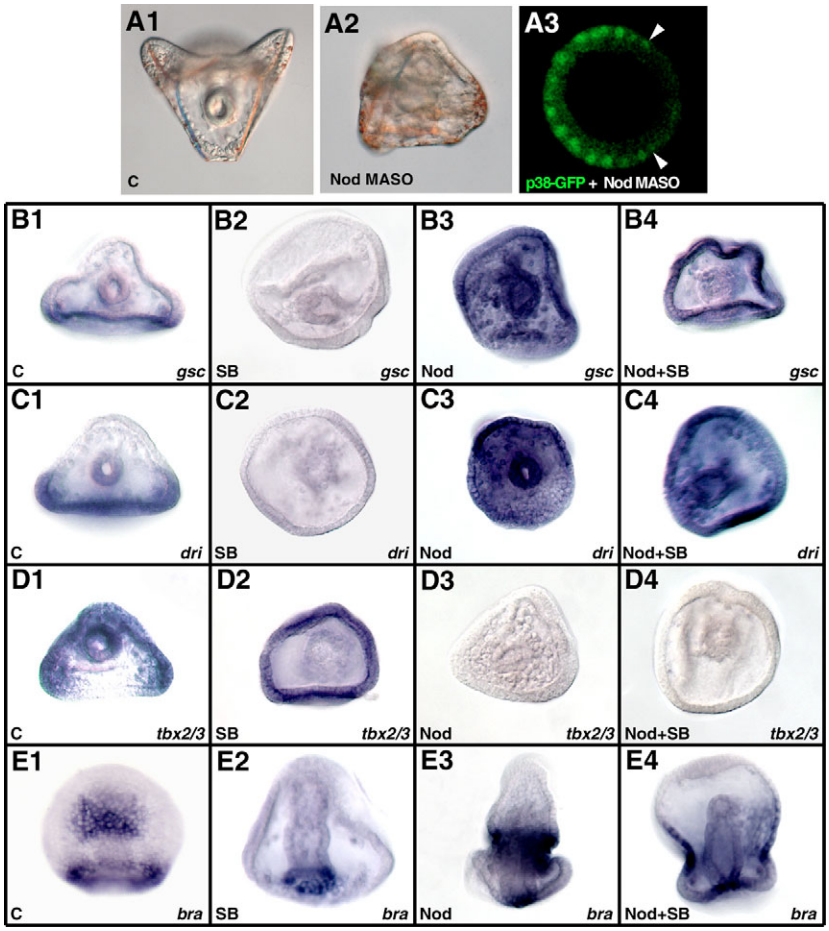

Fig. 6. Nodal expression oralizes embryos downstream from p38. (**A**) A1 and A2 show DIC images of a control embryo (A1) and an embryo injected with Nod MASO (0.7 mM, A2) at the pluteus stage. (A3) Embryo co-injected with Nod MASO and Lvp38-GFP, then imaged with live confocal microscopy at late blastula stage, as in Fig. 5C and 5E. (**B**-**E**) Whole-mount in situ analysis of Gsc (B), Dri (C), Tbx2/3 (D) and Bra (E) expression shown in control (1), SB-treated (2), Nod-injected (3), and Nod-injected plus SB-treated (4) embryos. Vegetal views are shown at prism stage, except for D (lateral views; D1 at late gastrula and D2-D4 at pluteus stage).

and skeletal abnormalities at pluteus stage (Fig. 6A2), consistent with the effects of anti-Nod MASO in other urchin species (Duboc et al., 2004; Flowers et al., 2004). To test whether Nodal participates in establishing the asymmetry of activated p38, Nod MASO and p38-GFP were co-injected and the embryos were evaluated using live confocal timecourses, as in Fig. 5. Asymmetric p38 clearance occurred normally (Fig. 6A3), demonstrating that Nodal is not involved in maintaining oral p38 activity. The aboral clearance appears to be somewhat more pronounced in comparison with the results in Fig. 5; however, this variation is within the range observed for these experiments. Thus p38 is required for Nodal expression, but Nodal is not involved in regulating the transient asymmetry of p38 activity.

To further test the hypothesis that p38 is upstream from Nodal, whole-mount in situ analysis was performed for oral and aboral gene expression in SB-treated embryos, LvNod-injected embryos, and embryos that received both treatments (Fig. 6B-E). SB-treated embryos did not express the oral genes LvGsc and LvDri (Fig. 6B2,C2), whereas the aboral gene Tbx2/3 was expressed uniformly (Fig. 6D2). LvBrachyury (Bra) is normally expressed in a vegetal ring corresponding to the blastopore, as well as in the presumptive stomadeum in the oral field (Fig. 6E1) (Croce et al., 2001; Gross and McClay, 2001). In SB-treated embryos, vegetal Bra expression was normal, but stomadeal expression was absent (Fig. 6E2). All of these results are consistent with aboralization in SB-treated embryos. LvNod-injected embryos show the opposite pattern, with ubiquitous expression of the oral genes Gsc, as expected (Duboc et al., 2004), and Dri (Fig. 6B3,C3), absent expression of the aboral gene Tbx2/3 (Fig. 6D3), and circumferential expression of stomadeal Bra (Fig. 6E3). These latter expression patterns were also observed in embryos that were both LvNod-injected and SB-treated (Fig. 6B4,C4,D4,E4). These results show that ubiquitous Nodal expression oralizes embryos even in the presence of the p38 inhibitor SB. Thus, Nodal functions downstream from p38.

A similar whole-mount in situ analysis was performed with Gsc injections (Fig. 7A-C). The results show that Gsc induced uniform expression of Dri (Fig. 7B3) and inhibited Tbx2/3 expression (Fig. 7C3), which is consistent with previous results in other sea urchin species (Amore et al., 2003; Croce et al., 2003). Gsc did not affect Nodal expression (Fig. 7A3), which is consistent with previous evidence that Gsc functions downstream from Nodal (Duboc et al., 2004). Embryos that were both Gsc-injected and SB-treated showed uniform Dri expression (Fig. 7B4) and no Tbx2/3 expression (Fig. 7C4). These data show that Gsc functions downstream from p38 with respect to these genes. These embryos showed no Nodal expression (Fig. 7A4), indicating that Gsc could not rescue Nodal expression downstream from p38, consistent with the relationship p38>Nodal>Gsc>Dri.

Embryos were stained for the aboral marker 1c10, which strongly labels SB-treated embryos (Fig. 7D2, see also Fig. 2B3), but does not label Gsc-injected embryos (Fig. 7D3), reflecting their aboralized and oralized phenotypes, respectively. If SB treatment aboralizes the embryo and Gsc drives oral specification downstream from p38, then one prediction is that in the presence of SB, Gsc expression in half of the embryo should oralize that half. Accordingly, one blastomere at

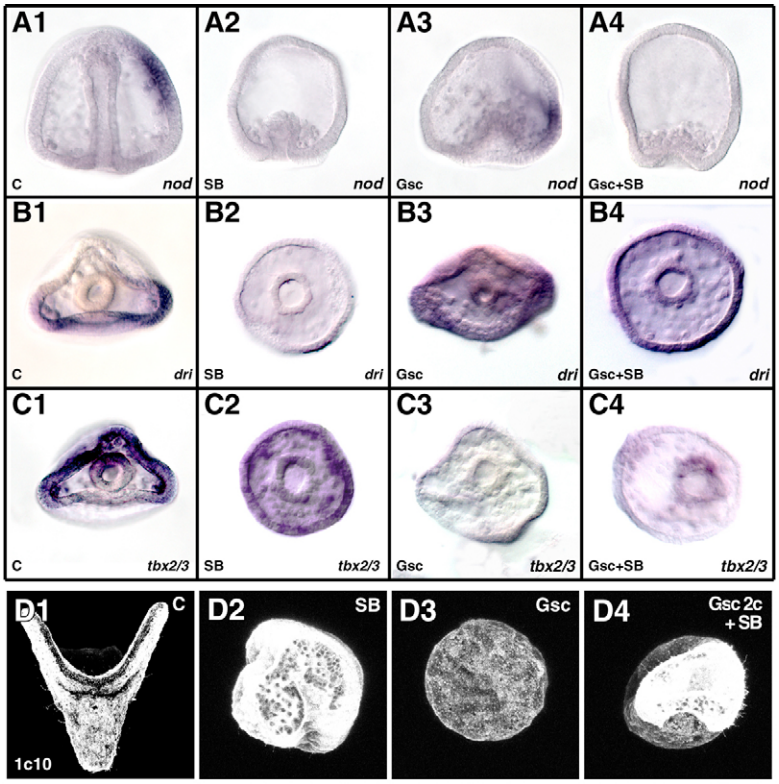

Fig. 7. LvGsc expression oralizes embryos downstream from p38. (**A**-**C**) Whole-mount in situ analysis of Nodal (A), Dri (B) and Tbx2/3 (C) expression in control (1), SB-treated (2), Gsc-injected (3), and Gsc-injected plus SB-treated (4) embryos. Vegetal views at prism stage are shown, except for A (lateral views at late gastrula). (**D**) Control (D1), SB-treated (D2), and Gsc-injected (D3) embryos stained with 1c10 at the pluteus stage. In D4, embryos were injected with Gsc in one blastomere at the 2-cell stage and then SB-treated and stained as in D1-D3. Full confocal projections are shown.

the 2-cell stage was injected with Gsc mRNA, and the embryos were treated with SB. In such embryos, 1c10 labeled only the uninjected side of the embryo (Fig. 7D4), consistent with this prediction. These results confirm that Gsc oralizes downstream from p38, and indicate that, when expressed asymmetrically, Gsc restores OA polarization in SB-treated embryos.

Asymmetrically expressed Gsc or Nodal rescue OA patterning downstream from p38

The results thus far have shown that Nodal and Gsc are each able to rescue the expression of oral markers downstream from p38. In addition, the data show that asymmetric Gsc expression can restore OA axis polarization in SB-treated embryos. It was unclear whether asymmetric Gsc also rescued axial patterning in these embryos (Fig. 7D4), as the recovery of patterning was obscured by the absence of skeletons. If skeletogenesis, but not patterning, could be restored in this context, then the effect on axial patterning could be determined. SB-wash treatment provided the necessary effect, as SB treatment until mesenchyme blastula stage (SB-wash) permits skeletogenesis but interferes with patterning (Fig. 4). Injections at the 2-cell stage provided the means to mimic the normal expression pattern of Gsc.

Injection of dye alone into one cell at the 2-cell stage did not restore patterning in SB-wash embryos (Fig. 8A). A similar 2-cell injection of Gsc mRNA in the absence of SB induced autonomous mispatterning on the injected side (Fig. 8B), whereas the uninjected side was patterned normally (compare with Fig. 3B4).

When LvGsc was injected at the 2-cell stage with SB-wash treatment, normal bilaterally symmetric patterning was produced in 69% of the resultant embryos (Fig. 8C), of which 100% expressed Gsc in the oral region (Fig. 8C3). Thus, asymmetrically expressed Gsc is functionally sufficient to restore both specification of the oral territory and patterning of the OA axis downstream from p38. This result also supports the hypothesis that the phenotype of SB-wash embryos (Fig. 4B) results from the delayed recovery of Gsc expression (Fig. 4C2), as spatially and temporally appropriate Gsc expression rescued that phenotype.

Because Gsc is downstream from Nodal, Nodal would be expected to also rescue axial patterning in this context. Indeed, 2-cell injection of LvNod followed by SB-wash treatment resulted in normally patterned skeletons with the same penetrance as LvGsc (Fig. 8D). In these embryos, the oral territory appeared to be expanded. This effect might be expected, as Nodal is a secreted protein that functions non-autonomously (Duboc et al., 2004). The 70% penetrance of rescue for both Nodal and Gsc may reflect a differential rescue depending on the orientation of the first cleavage plane, reported to divide left-right in about 70% of embryos (McCain and McClay, 1994; Summers et al., 1996). However, it is just as likely that the 70% rescue simply reflects the nominal success rate for this experimental system. In either case, these results indicate that the pathway Nodal>Gsc that operates in the oral ectoderm is sufficient to specify the oral territory and pattern the OA axis downstream from p38.

DISCUSSION

Axis specification often relies on the early asymmetric nuclearization of transcription factors across the embryo. In *Drosophila*, ventral nuclearization of Dorsal, an NFκB homolog, initiates specification of that territory, whereas in *Xenopus* and zebrafish, β-catenin nuclearization activates dorsal territory specification (Roth et al., 1989; Rushlow et al., 1989; Steward, 1989; Schneider et al., 1996). In the sea urchin, vegetal β-catenin nuclearization initiates specification of the vegetal territory (Wikramanayake et al., 1998; Logan et al., 1999). In each case, the transcription factor is sequestered from the nucleus until signals induce its relocalization.

The results of this study suggest that the specification of the OA axis in sea urchin embryos relies instead on the asymmetric nuclearization of a kinase, which, rather than being activated asymmetrically, is instead inactivated asymmetrically. In other organisms, p38 also plays asymmetric or polarizing roles during development. In *Drosophila*, blockade of the p38 pathway interferes with polarization of the egg through affects on both oskar localization and gurken expression, resulting in axial defects (Suzanne et al., 1999). In *Xenopus*, p38 is required for ventral specification of the ectoderm (Goswami et al., 2001), whereas in early zebrafish embryos, p38 is activated asymmetrically on the future dorsal side of the embryo (Fujii et al., 2000). Thus, p38 appears to function broadly in the animal kingdom in processes that define axial asymmetries.

This study relies extensively on the use of the p38 inhibitor SB, and therefore the specificity of this reagent is a crucial concern. Although we cannot rule out that SB interacts with other kinases in the sea urchin, several lines of evidence indicate that SB specifically inhibits Lvp38. Fig. 1A shows that the residues and secondary structural elements of human p38 that interact with SB are well conserved in Lvp38, suggesting that SB binds Lvp38 in a similar manner. Furthermore, the optimal dose of SB used in this study (20 μM) is consistent with doses used in mammalian systems (Rousseau et al., 2000; Takekawa et al., 2000), suggesting that SB binds to mammalian and *L. variegatus* p38 with similar affinities. In addition, there is a strong temporal agreement between the effects of SB treatment (Fig. 3) and the measures of p38 activity, particularly for the period of asymmetry (Fig. 5). Finally, and most importantly, dominant-negative p38 (KI-p38) phenocopies the effects of SB treatment with respect to morphology, aboralization, and the inhibition of Nodal and Gsc expression. Together, these data strongly suggest that SB inhibits Lvp38 in a specific manner.

The results show that p38 activity is upstream of Nodal expression, and is thus the earliest known protein functioning in OA axis specification in the sea urchin embryo. This conclusion is supported by several independent results. First, p38 activity is required for the expression of Nodal as assessed by both in situ hybridization and QPCR analysis. Second, Nodal is functionally downstream from p38, because Nodal induces oral specification and rescues axial patterning in the presence of SB. Third, Nodal does not feedback to activate p38, as antisense-mediated inhibition of Nodal did not perturb p38 activation or clearance. Taken together, these results show clearly that Nodal is downstream of p38.

The discrepancy between the timing of the onset of expression for Nodal in *L. variegatus* (late blastula) and *P. lividus* (60-cell stage) (Duboc et al., 2004) is most likely to be a species difference. Given the striking similarity of LvNodal and PlNodal function and morphology, this heterochronic difference seems relatively minor. In *P. lividus* embryos, it remains to be determined whether Nodal expression is p38 dependent at an earlier stage, or whether Nodal is activated by a different mechanism not involving p38. However, in *S. purpuratus* embryos, Nodal expression is abrogated by SB treatment, as it is in *L. variegatus* embryos (A. Poustka, personal communication), indicating that the relationship between p38 and Nodal described herein can be extended to at least one other cold-water urchin species.

The data indicate that p38 activity is required for Nodal transcription during the period of p38 asymmetric activation, as the asymmetry arises at 5.5 hpf as does the initiation of Nodal

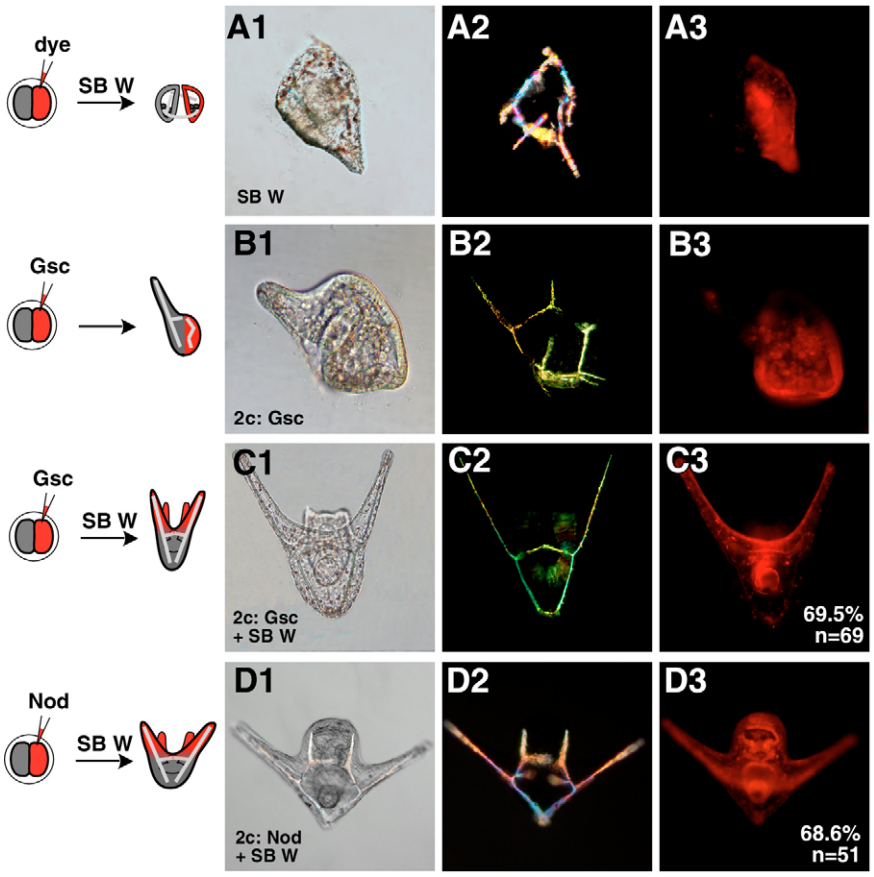

Fig. 8. Asymmetric expression of Gsc or Nodal restores oral-aboral patterning downstream from p38. The left column shows schematics representing the experiments for each panel. (**A**) SB-wash (SB W) treatment with a control 2-cell (2c) injection. (**B**) 2c Gsc injections without SB treatment. (**C**) 2c Gsc injections with SB-wash treatment. (**D**) 2c Nod injections with SB-wash treatment. Brightfield or DIC (1), skeletal (2) and fluorescence (3) images are shown.

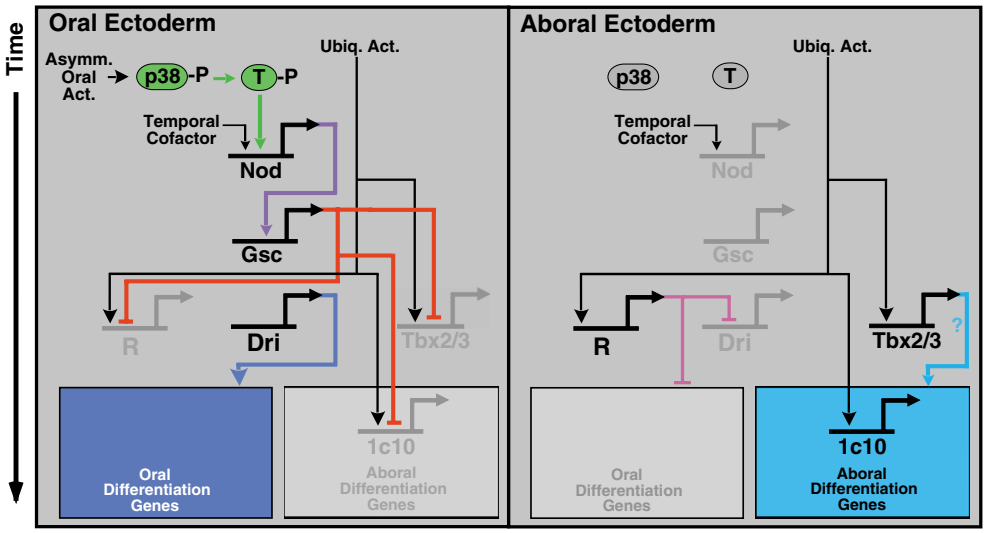

Fig. 9. Model summarizing the data presented. p38 is asymmetrically active on the future oral side of the embryo at late blastula stage, and initiates the expression of Nodal through an unknown intermediate transcription factor (T) that is a direct target of p38. The relationships between Nodal, Gsc, Dri and Tbx2/3 observed in *L. variegatus* are consistent with those observed in other species (Amore et al., 2003; Croce et al., 2003; Duboc et al., 2004). The induction of Dri is positioned downstream from Gsc via an intermediate repressor R, in keeping with the relationship observed in *S. purpuratus* embryos (Amore et al., 2003). Both Dri and Gsc are upstream from the oral differentiation genes, first because SpDri is necessary but not sufficient to induce oral-specific genes (Amore et al., 2003), and second because Gsc is sufficient for oralization downstream from p38 (Fig. 8C). Gsc is depicted as relieving the repression of the oral differentiation genes. A single repressor (R) is shown, although multiple repressors might exist. A single ubiquitous activator of aboral genes is shown in the aboral compartment for simplicity; there may of course be several. This activator may also induce the repressor/s of oral differentiation genes that is/are in turn repressed by Gsc. In the aboral ectoderm, the transcription factor Tbx2/3 might contribute to the induction of the aboral differentiation genes (Croce et al., 2003; Gross et al., 2003); the 1c10 antigen is expressed later in development and is thus likely to be an aboral differentiation gene.

expression. This hypothesis is strengthened by the timecourse data in Fig. 3, which show that oral specification becomes p38 independent at approximately 6 hpf, consistent with the end of the period of asymmetric p38 activity. If this is the case, then p38 must activate Nodal through at least one intermediate transcription factor that is a direct target of p38. Given the temporal proximity, a single intermediate factor is plausible. The expression of Nodal must additionally require a temporal cofactor, as p38 is active both before and during the period of asymmetry, whereas Nodal is not expressed before the asymmetry arises. The temporal factor need not be restricted spatially, as activated p38 provides spatial input. The intermediate transcription factor could also serve as the temporal factor if it were expressed only after the clearance of p38 had occurred, perhaps in response to the clearance-inducing event.

The results also show that p38 is required for Gsc expression, and that Gsc is sufficient for oralization downstream from p38. Gsc expression inhibited aboral Tbx2/3 and 1c10 expression, suggesting that Gsc may repress aboral genes in general, potentially explaining its ability to specify the oral territory. Given the complete oral rescue observed with asymmetric Gsc expression in SB-wash embryos (Fig. 8C), it seems reasonable to position Gsc at the top of the hierarchy of transcription factors that specify the oral ectoderm. Thus 'oral-ness' is apparently established primarily by transcriptional repression, as previously suggested (Angerer et al., 2001), a scenario similar to that observed in the specification of the PMC lineage, in which the induction of the transcriptional repressor Pmar1 relieves the repression of PMC specification genes (Oliveri et al., 2002). In the absence of p38 activity, aboral genes are uniformly expressed, suggesting that aboralization is the default ectodermal state in *L. variegatus*, similar to *S. purpuratus* (Wikramanayake et al., 1995). A ubiquitous activator (or activators) is thus likely to be responsible for the expression of aboral genes. One potential candidate is Otx2, a ubiquitous transcriptional activator that is known to induce aboral genes and to be competitively inhibited by Gsc (Mao et al., 1996; Li et al., 1999; Angerer et al., 2001). A model consistent with these results is shown in Fig. 9.

Several unresolved issues remain. One is the imperfect spatial congruence of P-p38 and Nodal expression at the time of clearance, as the domain of Nodal expression is coincident with, but smaller than, the region containing activated p38. This issue will likely be resolved by the identification of additional components in the OA gene regulatory network that function to refine the boundary of Nodal expression. A second issue is the mechanism underlying the clearance of p38. Resolving this will require learning how p38 is inactivated, whether by a phosphatase, degradation, or the modulation of nuclear import/export, as well as how that process is controlled both spatially and temporally. In addition, learning how p38 activity is maintained in the oral field will be of interest. The asymmetrically distributed mitochondria are suitably located to serve in this capacity, and, given the precedent of p38 activation in response to mitochondria (Ushio-Fukai et al., 1998; Kulisz et al., 2002; Lee et al., 2002), this will be an intriguing line of questioning to pursue.

The results of this study have supplied a molecular framework for OA specification and axial patterning. This will serve as a foundation for continued investigation into the molecular basis of these fundamental developmental events.

We thank E. Miranda, J. Dearing and T. Biondi for technical assistance; Drs J. Rast, C. Logan, R. Fehon and J. Croce for experimental suggestions; and Drs R. Angerer, L. Angerer, D. Sherwood and J. Croce for critical evaluation of the manuscript. This work was funded by NIH grants 61464, HD14483, and DOE grant DE-FG02-03ER63584. C.A.B. was partially supported by NRSA F32 HD41802-01.

References

Amore, G., Yavrouian, R. G., Peterson, K. J., Ransick, A., McClay, D. R. and Davidson, E. H. (2003). Spdeadringer, a sea urchin embryo gene required separately in skeletogenic and oral ectoderm gene regulatory networks. *Dev. Biol.* **261**, 55-81.

Angerer, L. M., Oleksyn, D. W., Levine, A. M., Li, X., Klein, W. H. and Angerer, R. C. (2001). Sea urchin goosecoid function links fate specification along the animal- vegetal and oral-aboral embryonic axes. *Development* **128**, 4393-4404.

Armstrong, N., Hardin, J. and McClay, D. R. (1993). Cell-cell interactions regulate skeleton formation in the sea urchin embryo. *Development* **119**, 833-840.

Bradham, C. A., Qian, T., Streetz, K., Brenner, D. A. and Lemasters, J. J. (1998). The mitochondrial permeability transition is required for TNFα-mediated apoptosis and cytochrome c release. *Mol. Cell. Biol.* **18**, 6353-6364.

Cameron, R. A., Leahy, P. S. and Davidson, E. H. (1996). Twins raised from separated blastomeres develop into sexually mature Strongylocentrotus purpuratus. *Dev. Biol.* **178**, 514-519.

Coffman, J. A., McCarthy, J. J., Dickey-Sims, C. and Robertson, A. J. (2004). Oral-aboral axis specification in the sea urchin embryo II. Mitochondrial distribution and redox state contribute to establishing polarity in Strongylocentrotus purpuratus. *Dev. Biol.* **273**, 160-171.

Corpet, F. (1988). Multiple sequence alignment with hierarchical clustering. *Nucl. Acids Res.* **16**, 10881-10890.

Croce, J., Lhomond, G. and Gache, C. (2001). Expression pattern of Brachyury in the embryo of the sea urchin Paracentrotus lividus. *Dev. Genes Evol.* **211**, 617-619.

Croce, J., Lhomond, G. and Gache, C. (2003). Coquillette, a sea urchin T-box gene of the Tbx2 subfamily, is expressed asymmetrically along the oral-aboral axis of the embryo and is involved in skeletogenesis. *Mech. Dev.* **120**, 561-572.

Davidson, E. H., Rast, J. P., Oliveri, P., Ransick, A., Calestani, C., Yuh, C. H., Minokawa, T., Amore, G., Hinman, V., Arenas-Mena, C. et al. (2002). A genomic regulatory network for development. *Science* **295**, 1669-1678.

Davies, S. P., Reddy, H., Caivano, M. and Cohen, P. (2000). Specificity and mechanism of action of some commonly used protein kinase inhibitors. *Biochem J.* **351**, 95-105.

Driesch, H. (1892). Entwicklungmechanische Studien III-VI. *Z. Wiss. Zool.* **55**, 160-184.

Duboc, V., Rottinger, E., Besnardeau, L. and Lepage, T. (2004). Nodal and BMP2/4 signaling organizes the oral-aboral axis of the sea urchin embryo. *Dev. Cell* **6**, 397-410.

Duboc, V., Rottinger, E., Lapraz, F., Besnardeau, L. and Lepage, T. (2005). Left-right asymmetry in the sea urchin embryo is regulated by nodal signaling on the right side. *Dev. Cell* **9**, 147-158.

Flowers, V. L., Courteau, G. R., Poustka, A. J., Weng, W. and Venuti, J. M. (2004). Nodal/activin signaling establishes oral-aboral polarity in the early sea urchin embryo. *Dev. Dyn.* **231**, 727-740.

Fujii, R., Yamashita, S., Hibi, M. and Hirano, T. (2000). Asymmetric p38 activation in zebrafish: its possible role in symmetric and synchronous cleavage. *J. Cell Biol.* **150**, 1335-1348.

Goswami, M., Uzgare, A. R. and Sater, A. K. (2001). Regulation of map kinase by the BMP-4/TAK1 pathway in *Xenopus* ectoderm. *Dev. Biol.* **236**, 259-270.

Gross, J. M. and McClay, D. R. (2001). The role of Brachyury (T) during gastrulation movements in the sea urchin Lytechinus variegatus. *Dev. Biol.* **239**, 132-147.

Gross, J. M., Peterson, R. E., Wu, S.-Y. and McClay, D. R. (2003). LvTbx2/3, a T-box family transcription factor involved in formation of the oral/aboral axis of the sea urchin embryo. *Development* **130**, 1989-1999.

Hardin, J., Coffman, J. A., Black, S. D. and McClay, D. R. (1992). Commitment along the dorsoventral axis of the sea urchin embryo is altered in response to $NiCl_2$. *Development* **116**, 671-685.

Kulisz, A., Chen, N., Chandel, N. S., Shao, Z. and Schumacker, P. T. (2002). Mitochondrial ROS initiate phosphorylation of p38 MAP kinase during hypoxia in cardiomyocytes. *Am. J. Physiol. Lung Cell. Mol. Physiol.* **282**, L1324-L1329.

Lee, J. C., Laydon, J. T., McDonnell, P. C., Gallagher, T. F., Kumar, S., Green, D., McNulty, D., Blumenthal, M. J., Heys, J. R., Landvatter, S. W. et al. (1994). A protein kinase involved in the regulation of inflammatory cytokine biosynthesis. *Nature* **372**, 739-746.

Lee, M. W., Park, S. C., Yang, Y. G., Yim, S. O., Chae, H. S., Bach, J. H., Lee, H. J., Kim, K. Y., Lee, W. B. and Kim, S. S. (2002). The involvement of reactive oxygen species (ROS) and p38 mitogen-activated protein (MAP) kinase in TRAIL/Apo2L-induced apoptosis. *FEBS Lett.* **512**, 313-318.

Li, X., Wikramanayake, A. H. and Klein, W. H. (1999). Requirement of SpOtx in cell fate decisions in the sea urchin embryo and possible role as a mediator of β-catenin signaling. *Dev. Biol.* **212**, 425-439.

Logan, C. Y. and McClay, D. R. (1997). The allocation of early blastomeres to the ectoderm and endoderm is variable in the sea urchin embryo. *Development* **124**, 2213-2223.

Logan, C. Y., Miller, J. R., Ferkowicz, M. J. and McClay, D. R. (1999). Nuclear β-catenin is required to specify vegetal cell fates in the sea urchin embryo. *Development* **126**, 345-357.

Malinda, K. M. and Ettensohn, C. A. (1994). Primary mesenchyme cell migration in the sea urchin embryo: distribution of directional cues. *Dev. Biol.* **164**, 562-578.

Mao, C. A., Wikramanayake, A. H., Gan, L., Chuang, C. K., Summers, R. G. and Klein, W. H. (1996). Altering cell fates in sea urchin embryos by overexpressing SpOtx, an orthodenticle-related protein. *Development* **122**, 1489-1498.

McCain, E. R. and McClay, D. R. (1994). The establishment of bilateral asymmetry in sea urchin embryos. *Development* **120**, 395-404.

Oliveri, P., Carrick, D. M. and Davidson, E. H. (2002). A regulatory gene network that directs micromere specification in the sea urchin embryo. *Dev. Biol.* **246**, 209-228.

Raingeaud, J., Gupta, S., Rogers, J. S., Dickens, M., Han, J., Ulevitch, R. J. and Davis, R. J. (1995). Pro-inflammatory cytokines and environmental stress cause p38 mitogen-activated protein kinase activation by dual phosphorylation on tyrosine and threonine. *J. Biol. Chem.* **270**, 7420-7426.

Raingeaud, J., Whitmarch, A. J., Barrett, T., Derigard, B. and Davis, R. (1996). MKK3- and MKK6-regulated gene expression is mediated by the p38 mitogen-activated protein kinase signal transduction pathway. *Mol. Cell. Biol.* **16**, 1247-1255.

Rast, J. P., Amore, G., Calestani, C., Livi, C. B., Ransick, A. and Davidson, E. H. (2000). Recovery of developmentally defined gene sets from high-density cDNA macroarrays. *Dev. Biol.* **228**, 270-286.

Roth, S., Stein, D. and Nusslein-Volhard, C. (1989). A gradient of nuclear localization of the dorsal protein determines dorsoventral pattern in the Drosophila embryo. *Cell* **59**, 1189-1202.

Rousseau, S., Houle, F., Kotanides, H., Witte, L., Waltenberger, J., Landry, J. and Huot, J. (2000). Vascular endothelial growth factor (VEGF)-driven actin-based motility is mediated by VEGFR2 and requires concerted activation of stress-activated protein kinase 2 (SAPK2/p38) and geldanamycin-sensitive phosphorylation of focal adhesion kinase. *J. Biol. Chem.* **275**, 10661-10672.

Rushlow, C. A., Han, K., Manley, J. L. and Levine, M. (1989). The graded distribution of the dorsal morphogen is initiated by selective nuclear transport in Drosophila. *Cell* **59**, 1165-1177.

Schier, A. F. and Shen, M. M. (2000). Nodal signalling in vertebrate development. *Nature* **403**, 385-389.

Schneider, S., Steinbeisser, H., Warga, R. M. and Hausen, P. (1996). Beta-catenin translocation into nuclei demarcates the dorsalizing centers in frog and fish embryos. *Mech. Dev.* **57**, 191-198.

Shi, Y. and Gaestel, M. (2002). In the cellular garden of forking paths: how p38 MAPKs signal for downstream assistance. *Biol. Chem.* **383**, 1519-1536.

Steward, R. (1989). Relocalization of the dorsal protein from the cytoplasm to the nucleus correlates with its function. *Cell* **59**, 1179-1188.

Summers, R. G., Piston, D. W., Harris, K. M. and Morrill, J. B. (1996). The orientation of first cleavage in the sea urchin embryo, Lytechinus variegatus, does not specify the axes of bilateral symmetry. *Dev. Biol.* **175**, 177-183.

Suzanne, M., Irie, K., Glise, B., Agnes, F., Mori, E., Matsumoto, K. and Noselli, S. (1999). The Drosophila p38 MAPK pathway is required during oogenesis for egg asymmetric development. *Genes Dev.* **13**, 1464-1474.

Takekawa, M., Adachi, M., Nakahata, A., Nakayama, I., Itoh, F., Tsukuda, H., Taya, Y. and Imai, K. (2000). p53-inducible wip1 phosphatase mediates a negative feedback regulation of p38 MAPK-p53 signaling in response to UV radiation. *EMBO J.* **19**, 6517-6526.

Tong, L., Pav, S., White, D. M., Rogers, S., Crane, K. M., Cywin, C. L., Brown, M. L. and Pargellis, C. A. (1997). A highly specific inhibitor of human p38 MAP kinase binds in the ATP pocket. *Nat. Struct. Biol.* **4**, 311-316.

Ushio-Fukai, M., Alexander, R. W., Akers, M. and Griendling, K. K. (1998). p38 Mitogen-activated protein kinase is a critical component of the redox-sensitive signaling pathways activated by angiotensin II. Role in vascular smooth muscle cell hypertrophy. *J. Biol. Chem.* **273**, 15022-15029.

Wang, Z., Canagarajah, B. J., Boehm, J. C., Kassisa, S., Cobb, M. H., Young, P. R., Abdel-Meguid, S., Adams, J. L. and Goldsmith, E. J. (1998). Structural basis of inhibitor selectivity in MAP kinases. *Structure* **6**, 1117-1128.

Wikramanayake, A. H., Brandhorst, B. P. and Klein, W. H. (1995). Autonomous and non-autonomous differentiation of ectoderm in different sea urchin species. *Development* **121**, 1497-1505.

Wikramanayake, A. H., Huang, L. and Klein, W. H. (1998). β-Catenin is essential for patterning the maternally specified animal-vegetal axis in the sea urchin embryo. *Proc. Natl. Acad. Sci. USA* **95**, 9343-9348.

Young, P. R., McLaughlin, M. M., Kumar, S., Kassis, S., Doyle, M. L., McNulty, D., Gallagher, T. F., Fisher, S., McDonnell, P. C., Carr, S. A. et al. (1997). Pyridinyl imidazole inhibitors of p38 mitogen-activated protein kinase bind in the ATP site. *J. Biol. Chem.* **272**, 12116-12121.